

This article was downloaded by:

On: 25 January 2011

Access details: *Access Details: Free Access*

Publisher *Taylor & Francis*

Informa Ltd Registered in England and Wales Registered Number: 1072954 Registered office: Mortimer House, 37-41 Mortimer Street, London W1T 3JH, UK



Separation Science and Technology

Publication details, including instructions for authors and subscription information:

<http://www.informaworld.com/smpp/title~content=t713708471>

Volume Flow Resistance of a Hemodialysis Membrane and Protein Adsorption

C. Fabiani^a; M. Pizzichini^a; S. Bersani^a; C. U. Casciani^b; S. Digiulio^b; P. L. Fortezza^b; A. Maldonato^c; M. Pittaluga^c

^a DIVISIONE CHIMICA, E.N.E.A., ROME, ITALY ^b UNIVERSITÁ ROMA II TOR VERGATA CATTEDERA DI MEDICINA, ROME, ITALY ^c UNIVERSITÁ ROMA I LA SAPIENZA IST. II CLINICA MEDICA, ROME, ITALY

To cite this Article Fabiani, C. , Pizzichini, M. , Bersani, S. , Casciani, C. U. , Digiulio, S. , Fortezza, P. L. , Maldonato, A. and Pittaluga, M.(1990) 'Volume Flow Resistance of a Hemodialysis Membrane and Protein Adsorption', *Separation Science and Technology*, 25: 5, 593 — 608

To link to this Article: DOI: [10.1080/01496399008050352](https://doi.org/10.1080/01496399008050352)

URL: <http://dx.doi.org/10.1080/01496399008050352>

PLEASE SCROLL DOWN FOR ARTICLE

Full terms and conditions of use: <http://www.informaworld.com/terms-and-conditions-of-access.pdf>

This article may be used for research, teaching and private study purposes. Any substantial or systematic reproduction, re-distribution, re-selling, loan or sub-licensing, systematic supply or distribution in any form to anyone is expressly forbidden.

The publisher does not give any warranty express or implied or make any representation that the contents will be complete or accurate or up to date. The accuracy of any instructions, formulae and drug doses should be independently verified with primary sources. The publisher shall not be liable for any loss, actions, claims, proceedings, demand or costs or damages whatsoever or howsoever caused arising directly or indirectly in connection with or arising out of the use of this material.

Volume Flow Resistance of a Hemodialysis Membrane and Protein Adsorption

C. FABIANI, M. PIZZICHINI, and S. BERSANI

E.N.E.A., DIVISIONE CHIMICA
CRE-CASACCIA, ROME, ITALY

C. U. CASCIANI, S. DIGIULIO, and P. L. FORTEZZA

UNIVERSITÁ ROMA II TOR VERGATA
CATTEDRA DI MEDICINA, ROME, ITALY

A. MALDONATO and M. PITTALUGA

UNIVERSITÁ ROMA I LA SAPIENZA
IST. II CLINICA MEDICA, ROME, ITALY

Abstract

Polarization and adsorption effects during bovine serum albumin (BSA) ultrafiltration across a commercial hemodialysis membrane are discussed. BSA adsorption on the membrane surface depends on the pH and concentration of solutions. Overall membrane permeability is reduced due to the resistance of both the concentration polarization and the adsorption layers. Ultrafiltration experiments with a pure solvent (water) and solutions allow the different contributions to the total volume flow resistance of the membrane to be distinguished. These data are needed to develop a model bioartificial pancreas in which animal pancreatic islets of Langerhans are bounded between two ultrafiltration membranes.

INTRODUCTION

The ultrafiltration of protein solutions and the effects of membrane polarization and protein adsorption have been widely investigated

because of the practical importance of these phenomena in dairy and pharmaceutical industries, biotechnology, and biomedicine (1-3). In the field of artificial organs, several research groups (4-7) have undertaken the study of a bioartificial pancreas in which ultrafiltration membranes will play an important role.

By implantable bioartificial pancreas (IBP) we mean an implantable device for producing and releasing insulin in a controlled way in the blood system as a consequence of an increase in blood glucose content. The device is based on the transplantation of nonsyngeneic islets of Langerhans in a diabetic host. Immune rejection is avoided with artificial membranes which separate islets and blood. This device, schematically shown in Fig. 1, is subject to many severe operating conditions (5). A complete transient steady-state model (5-7) is needed not only to verify its performance but also to take into account the possible time variation of islets activity, membrane performance, and hydrodynamic conditions.

The conceptual design of the biopancreas assumes that blood flow at arterial pressure into the ultrafiltration cell across two channels at different pressures. This effect is produced by the difference between the arterial and venous pressure (at which blood leaves the cell) and the two distributed pressure resistances (Fig. 1).

The pressure difference between the upper and lower part of the cell determines the production of an ultrafiltrate which crosses the layer formed by the two membranes where islets of Langerhans are confined.

The glucose transported by the ultrafiltrate stimulates the islets, and insulin is produced and transported out of the cell in the vein. Therefore, no external driving force (pressure difference) must be provided to operate the biopancreas.

The kinetic response of the biopancreas (5-7) (that is, the delay between the increase in blood glucose content and the maximum insulin release) depends on many geometrical, hydrodynamic, and transport parameters, and among them the permeability of the membranes is important. The permeability of the two membranes can change during the operation of the device because of polarization and adsorption phenomena, and these changes can produce different effects on the high pressure and low pressure membranes.

The use of heparin is necessary in the practical operation of the device, and this introduces further complexity to the system. A complete study of these changes is needed to develop a reliable model of the biopancreas.

In this paper, adsorption and polarization phenomena occurring when BSA solutions are ultrafiltrated across polyacrylonitrile Hospital PAN membranes are discussed.

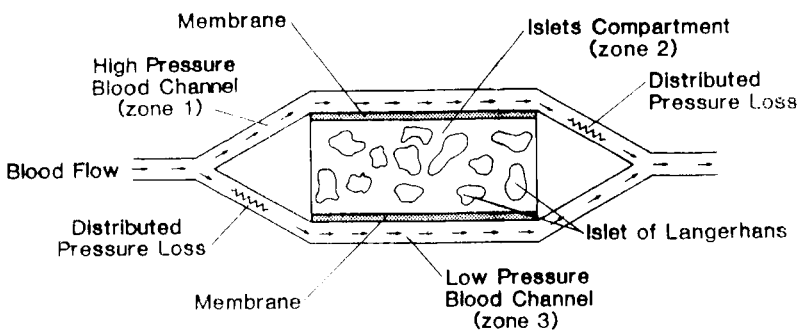


FIG. 1. Ideal sketch of a bioartificial pancreas based on islets of Langerhans confinement between two ultrafiltration membranes.

Membranes were chosen from among those widely used in hemofiltration.

BSA molecules are assumed to mimic the behavior of human albumin which represents the higher protein content of the blood. The effects of other blood constituents will be studied separately.

PROTEIN ULTRAFILTRATION

Protein molecules adsorb on membrane surfaces both under static (batch) and dynamic (ultrafiltration) conditions. Protein molecular charge, membrane surface charge, and the protein structure at the interfacial solution-membrane layer are factors which affect membrane permeability.

A concentration polarization gradient of retained molecules is formed at the solution-membrane boundary layer, and macromolecules can be deposited or adsorbed on the membrane surface during ultrafiltration.

The transport of a solution across a membrane experiences hydraulic resistance in both the boundary layer and the adsorbed layer. This resistance increases the membrane volume flow resistance. Solution transport is also affected by a decrease in the effective transmembrane pressure difference due to the osmotic pressure difference produced by the interfacial concentration gradient. The dynamic situation is sketched in Figs. 2 and 3.

The volume flow, J_v , observed when pure solvent is ultrafiltrated across a membrane with a P pressure difference follows Darcy's law:

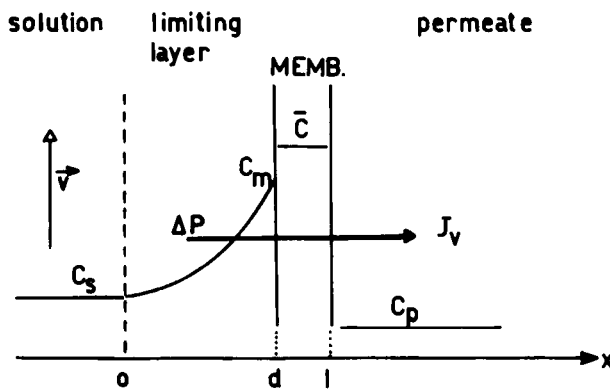


FIG. 2. Concentration profiles during the ultrafiltration of a solution containing macromolecules which can adsorb (\bar{c}) on the membrane.

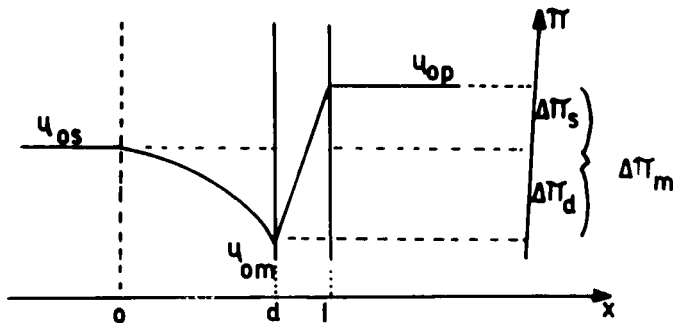


FIG. 3. Water chemical potential and corresponding osmotic pressure effect relative to a concentration gradient pattern as reported in Fig. 2.

$$J_v = \Delta P / \eta R_m \quad (1)$$

where R_m is the membrane hydraulic resistance and η is the solvent viscosity. When a protein solution is ultrafiltrated, the volume permeability decreases because of polarization and adsorption phenomena.

The flux-pressure relationship is not linear (2). With reference to Figs. 2 and 3 and assuming steady state, i.e., $J_v = \text{constant}$, the flux-pressure

relationship can be written in different ways according to the assumed "effective" driving force ΔP^* :

$$(A) \quad \Delta P^* = \Delta P - \Delta \pi_s \quad (2)$$

where $\Delta \pi_s$ is the difference in osmotic pressure between the solution and the permeate. The volume flow is then given by

$$(3) \quad J_v = (\Delta P - \Delta \pi_s)/\eta_1(R_m^* + R_d)$$

where η_1 is the average solution viscosity in the concentration range of the fed solution and permeate, and R_m^* and R_d are the membrane (including the possible contribution of the adsorbed layer, R_a) and the boundary layer resistances, respectively.

$$(B) \quad \Delta P^* = \Delta P - \Delta \pi_d \quad (4)$$

where $\Delta \pi_d$ is the osmotic pressure difference between the solution and the solution-membrane interfacial layer (where the protein concentration is c_m). In this case

$$(5) \quad J_v = (\Delta P - \Delta \pi_d)/\eta_2 R_d$$

where η_2 is the average viscosity of the solution in the boundary layer concentration gradient.

$$(C) \quad \Delta P^* = \Delta P - \Delta \pi_m \quad (6)$$

where $\Delta \pi_m$ is the osmotic pressure difference between the two membrane surfaces. Therefore,

$$(7) \quad J_v = (\Delta P - \Delta \pi_m)/\eta_3 R_m^*$$

where η_3 is the permeate viscosity assumed equal to that of the membrane pore solution.

Equations (3), (5), and (7) are different formulations of the same transport phenomena (in the frame of the osmotic polarization model) and do not represent distinct models for volume transport. They are essentially three different definitions of the specific hydraulic resistance: the total membrane plus the resistance shown by the diffuse interfacial polarized layer ($R_m^* + R_d$) if the resistance of the adsorbed protein layer is

included in R_m^* ; the simple interfacial polarization layer resistance R_d ; and the total membrane plus adsorbed layer resistance R_m^* . Therefore, by measuring the volume flow at a given applied external pressure, it is possible to calculate a given set of volume resistances according to the choice of osmotic contribution to correct the applied pressure driving force to the effective pressure driving force. The three equations contain different viscosity terms which take into account the changes of composition of the solution which flows across the asymmetric interface between the two bulk solutions and the possible effects of the microenvironment (viscosity of the membrane pore solution). If the three different osmotic correction terms and the three different viscosities are known from experiments or calculated, measurement of the volume ultrafiltration flow will allow determination of all the volume resistances of the membrane system: the interfacial polarization layer, the adsorbed layer, and the pure membrane resistances.

However, a simplified procedure is possible if only the pure membrane and the adsorbed protein layer resistances are evaluated. The membrane is coated with the protein adsorbed layer by performing suitable ultrafiltration experiments with protein solutions. The solution is changed, and a pure solvent is ultrafiltrated through the coated membrane. In this case the osmotic correction is zero, and the resistance of the coated membrane is the sum of the pure membrane resistance and the resistance of the adsorbed protein layer according to Eq. (7), where $\eta_1 = \eta_3$ (pure solvent). If the pure membrane resistance is separately measured by ultrafiltrating the solvent across the clean membrane, both the R_m and R_d contributions can be obtained.

This paper presents the results obtained with BSA solutions (which simulate the blood albumin in both concentration and pH) in contact with Hospal's polyacrylonitrile membranes. In Table 1 the main features of BSA and Hospal's membrane are collected.

EXPERIMENTAL

Solutions with pH in the 2-8 range have been obtained with carbonate, phosphate, and citrate buffers by using analytical grade reagents. BSA was a Merck product with a purity higher than 90%. Solutions in the 5-50 g/L concentration range were used.

The protein concentration was measured spectrophotometrically at 235 nm by using a specific calibration curve or by Lowry's method at 750 nm in the 5-25 g/L range and at 500 nm with more concentrated solutions.

TABLE 1
Characteristics of BSA Molecules and Hospital Membrane

Protein: Bovine Serum Albumin		
Molecular weight	69.000	
Geometry (8)	Globular	
	Ellipsoid	$a = 70.5 \text{ \AA}$
	Spherical radius	$b = 20.8 \text{ \AA}$ $r = 31.3 \text{ \AA}$
	Molecular volume	$v_m = 1.5 \times 10^{-19} \text{ cm}^3$
Electrical properties (8)	Isoelectric point (NaCl 0.15 M)	pH 4.72
	Isotonic point (NaCl 0.15 M)	pH 5.22-5.55
	Charge number	-20.4, pH 7.4 -9.1, pH 5.4 +4.5, pH 4.5
Diffusion coefficient (D) (pH 7.2, $c = 12 \text{ g/L}$, $T = 25^\circ\text{C}$)	$D = 7.0 \times 10^{-11} \text{ m}^2/\text{s}$	
Membrane: Polyacrylonitrile		
Thickness	$4 \times 10^{-5} \text{ m}$	
Porosity	0.5	
Cut-off	10,000	

Permeability measurements were performed with the apparatus shown in Fig. 4 by using flat Perspex cells (Fig. 5). Membranes with two different surface areas (11.9 and 70 cm^2) were mounted. Ultrafiltration experiments were made with a differential pressure of 24.133 kPa, equivalent at 0.238 atm. The system was thermostated at 23°C .

In some experiments, after the deposition of a BSA layer on the membrane surface, the quantity of deposited protein was measured. This was done by soaking the membrane coated with the protein layer in $20-50 \text{ cm}^3$ of a 1% solution of TWEEN 20 surfactant for 24 h under stirring and at a controlled temperature (between 30 and 40°C). The proteins in solution were then measured. The experimental cell for ultrafiltration experiments was operated with feed recirculating flows corresponding to a linear velocity in the $1.5-3.0 \text{ cm/s}$ range through a rectangular feed chamber of $1.5 \times 5 \text{ cm}^2$ cross section. The resultant Reynolds numbers, calculated from the water viscosity and the solution densities, fall in the 57-80 range typical of laminar flow.

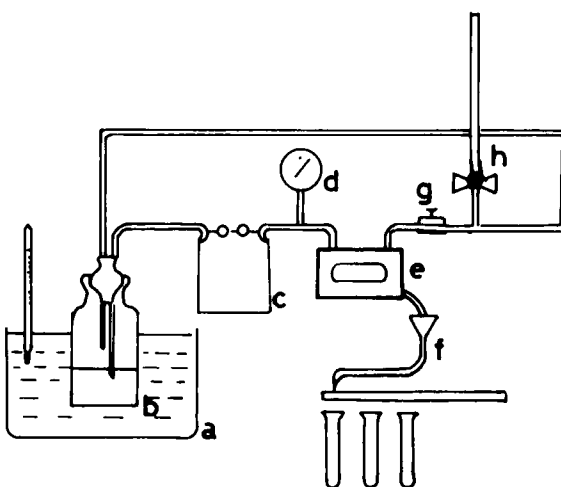


FIG. 4. Sketch of the experimental assembly for volume flow measurements in ultrafiltration experiments: (a) thermostat, (b) feed solution, (c) pump, (d) manometer, (e) ultrafiltration cell, (f) fraction collector, (g) pressure regulation, (h) flowmeter.

RESULTS

The volume fluxes obtained under the reported experimental conditions are constant in time, showing good membrane compaction and stability. The volumes collected as a function of time during the ultrafiltration of solvent (water), buffer solutions, and BSA solutions at different concentrations are reported in Fig. 6. The slope of the permeation plots decreases when the solution concentration increases, showing there is increased membrane resistance. Under the reported experimental conditions it can be assumed that membrane polarization occurs when ultrafiltration starts.

By means of Eq. (1) and the data corresponding to the ultrafiltration of pure water, the membrane resistance, R_m , can be calculated. On the other hand, due to the unknown value of the effective pressure differential, the resistance of the protein solution cannot be evaluated. Permeation plots for the ultrafiltration of pure water across membranes which have previously ultrafiltrated BSA solutions of different concentrations are reported in Fig. 7. The lower value of water permeability indicates that the

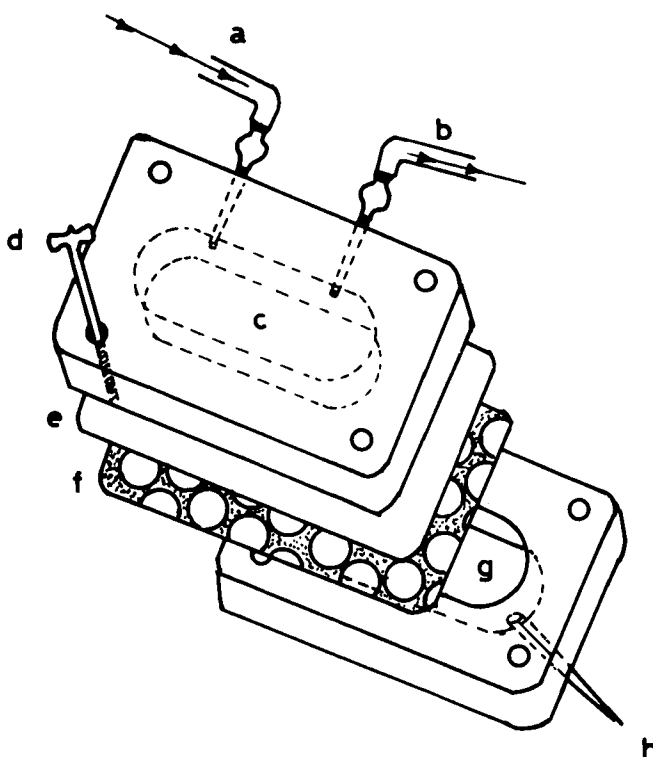


FIG. 5. View of the ultrafiltration cell: (a) feed input, (b) feed recirculation, (c) ultrafiltration chamber, (d) screw, (e) membrane, (f) screen for membrane support, (g) permeate collection, (h) permeate output.

polarization observed during protein ultrafiltration (Fig. 6) is maintained.

We conclude that an irreversible resistance effect occurs because of protein adsorption on the membrane surface. The total membrane resistance (polymer plus adsorption layer) is stable, and the fluxes obtained are constant.

The data of Fig. 7 correspond to Eq. (7) by setting $\Delta\pi_m = 0$ (ultrafiltration of pure solvent; $\eta_1 = \eta_3$):

$$\eta_1 J_{v3} = \Delta P / R_m^* \quad (8)$$

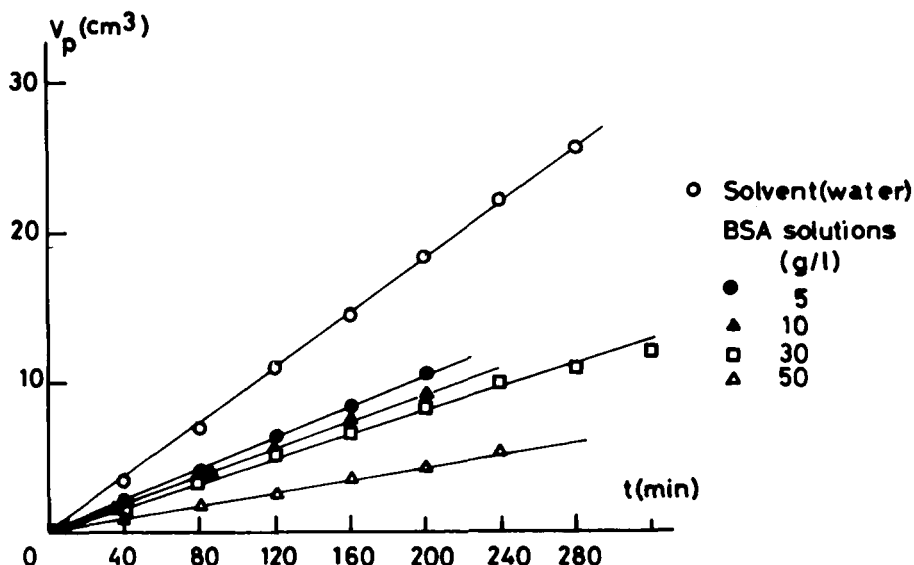


FIG. 6. Permeate volume, V_p , versus time when pure solvent (water) and BSA solutions are ultrafiltrated across polyacrylonitrile membranes: $\text{pH} = 6.88$, $T = 23^\circ\text{C}$, $\Delta P = 3.5$ psi.

Also, from Fig. 7 plots and Eq. (1), the membrane resistance for as-received polymer and pure solvent transport, R_m , can be calculated, and from these values the membrane resistance due to the adsorbed layer, R_a , can be obtained from Eq. (8):

$$R_a = (\Delta P/\eta_1)(1/J_{v3} - 1/J_{v1}) \quad (9)$$

where 1 is the index for water ultrafiltration across a clean membrane and 3 is the index for water ultrafiltration through a membrane with adsorbed protein. When R_a and R_m are known, the reduction in applied pressure due to osmotic effects at the membrane-solution interface can be calculated. From Eqs. (1) and (7),

$$\Delta\pi_m = \Delta P(1 - n_3 J_{v3}/n_1 J_{v2}) \quad (10)$$

where index 2 refers to the ultrafiltration of BSA solutions. In Eq. (10), because BSA is retained by the membrane, the viscosities of the permeate liquids have been assumed equal to the solvent viscosity ($\eta_1 = \eta_3$).

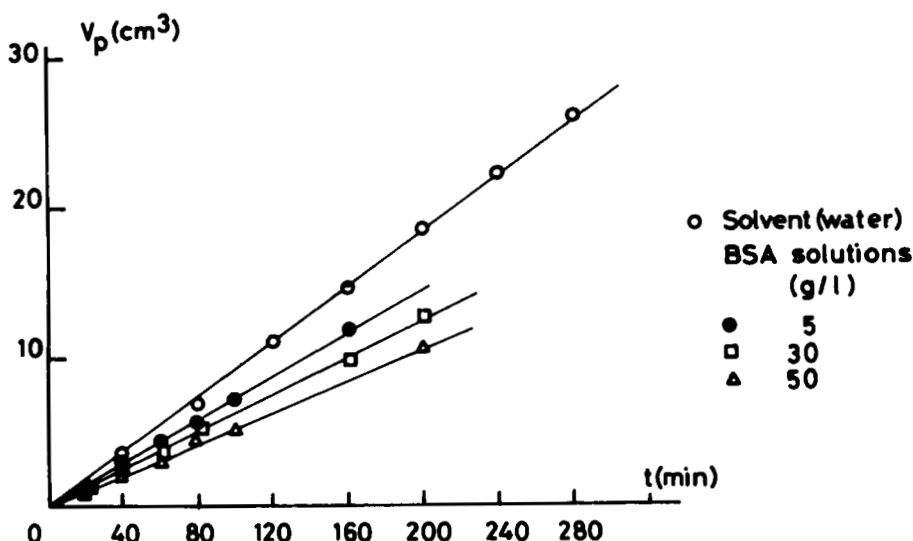


FIG. 7. Water permeation across polyacrylonitrile membranes when they are used as received or after pre-equilibration with BSA solutions of different concentrations: pH 6.88, $\Delta P = 3.5$ psi, $T = 23^\circ\text{C}$.

The results of the above calculations are collected in Table 2. The viscosity of water has been used: $\eta_1 = 8.94 \times 10^{-4} \text{ Pa} \cdot \text{s}$. The protein interfacial concentration, c , can be written in the steady state as a function of the volume flow. Under complete protein rejection and steady-state conditions, the convective flow is balanced by the diffusive transport in the boundary limit layer:

$$cJ_v = D \frac{dc}{dx} \quad (11)$$

By integrating between $x = 0$, $c = c_s$, and $x = d$, $c = c_m$, we get

$$c_m = c_s \exp(J_v/k) \quad (12)$$

where $k = D/d$ is the average protein diffusion coefficient, and D is the average protein diffusion coefficient in the limit-layer concentration gradient. The above relations allow the hydraulic resistance values and the interfacial concentration of the rejected macromolecules to be obtained from flux measurements performed under different conditions.

TABLE 2

Membrane, R_m , and Adsorbed Layer, R_a , Resistances and Osmotic Pressure Difference $\Delta\pi_m$ across the Membrane. Polyacrylonitrile Membrane: $\Delta P = 24.1233$ kPa, $T = 23^\circ\text{C}$, pH 6.88

c_s (k/m ³)	J_{v3} (m/s) $\times 10^{-7}$	R_m^* (m ⁻¹) $\times 10^{13}$	R_a (m ⁻¹) $\times 10^{13}$	J_{v2} (m/s) $\times 10^{-7}$	$\Delta\pi_m$ (Pa) $\times 10^3$
0	12.7 (= J_{v1})	2.13 (= R_m)	—	—	—
5	10.1	2.68	0.55	7.3	6.69
10	9.8	2.76	0.63	6.5	8.13
30	8.7	3.08	0.95	5.9	7.77
50	7.0	3.86	1.73	3.0	13.79

The osmotic pressure of BSA solutions as a function of pH and concentration are known from the literature (8, 9). The following function, obtained by Vilker et al. (8) at 25°C and pH 7.4, can be used in the 0–500 g/L concentration range:

$$\pi = (RT/M)(c + Ac^2 + Bc^3) + RT\{2[(Zc/2M) + m^2]\}^{1/2} - 2m \quad (13)$$

where Z is the charge of a polymer of M molecular weight at concentration c in a saline solution of molarity m , and A and B are adjusting parameters. If the m values from Eq. (13) are known (Table 2), the interfacial protein concentration can be obtained. For concentrations below 100 g/L, a good approximation to Eq. (13) is the ideal van't Hoff equation: $\pi/c = RT/M$.

If interfacial concentration and the adsorption isotherm are known, the surface membrane concentration of the protein adsorbed layer can be calculated. For BSA adsorption on a different membrane made from the same polymer as the one used in this study (3), the following isotherm of the Freundlich type has been used:

$$c_{ae} = 0.09c_m^{0.65} \quad (\text{pH 7.2}) \quad (14)$$

The data of Table 3 were obtained according to the previous discussion.

From the data of Table 3 it can be deduced that concentration polarization produces high interfacial concentrations, even when the protein solution is ultrafiltrated at low pressure, provided the membrane (as in the Hospal membrane case) has high volume permeability. In fact, Eq. (9)

TABLE 3

Interfacial Concentration, c_m , and Equilibrium Concentration of the Adsorbed Layer, c_{ae} , for Polyacrylonitrile Membranes Exposed to BSA Solutions. $T = 23^\circ\text{C}$, pH 6.88

c_s (kg/m ³)	R_a (m ⁻¹) × 10 ¹³	c_m (kg/m ³)	c_{ae} (kg/m ²) × 10 ⁻³
5	0.55	186.3	2.7
10	0.63	226.4	3.1
30	0.95	216.4	3.0
50	1.73	384.1	4.3

shows that the interfacial concentration at given fixed conditions rises exponentially with the volume flux, J_v .

From Eq. (12), if the protein diffusion coefficient is available (for BSA, $D = 7 \times 10^{-11}$ m²/s), the thickness d of the boundary limit layer can be calculated with the mass-transfer coefficient value k :

$$k = D/d = J_{v2}/\ln (c_m/c_s) \quad (15)$$

These mass transfer coefficients, as reported in the Experimental section, correspond to Reynolds numbers in the 57–80 range for the feed flow rate. (See Table 4.)

pH Effect

The BSA isoelectric point is pH 4.7, and for this value the lowest electrostatic protein-membrane interaction is expected. Therefore, the pH of

TABLE 4

Mass-Transfer Coefficient, k , and Boundary Limit Layer Thickness d . Same Conditions as in Table 2

c_s (kg/m ³)	c_m (kg/m ³)	J_{v2} (m/s) × 10 ⁻⁷	k (m/s) × 10 ⁻⁷	d (m) × 10 ⁻⁴
5	186	7.4	2.06	3.4
10	226	6.1	1.97	3.6
30	216	5.0	2.54	2.8
50	384	3.0	1.47	4.8

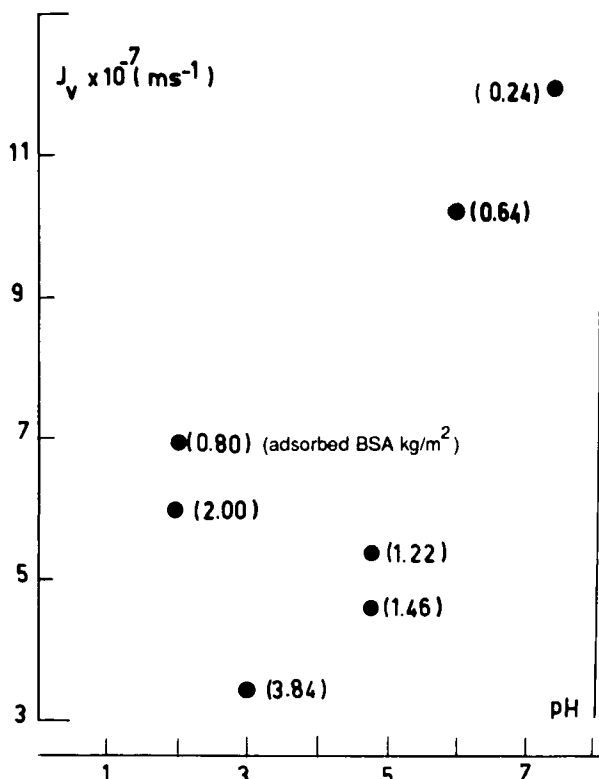


FIG. 8. Steady-state ultrafiltration volume flow for BSA solutions of 5 g/L at different pH values: $\Delta P = 3.5$ psi, $T = 23^\circ C$.

a BSA solution affects protein adsorption and membrane permeability. In Fig. 8 the membrane permeabilities for the ultrafiltration of 5 g/L BSA solutions at different pH values are shown together with the protein adsorbed. These data were obtained after each ultrafiltration run by treating the membrane with the TWEEN 20 surfactant and measuring the concentration of the dissolved protein. pH and ionic strength effects on protein ultrafiltration cannot be fully explained by electrostatic interactions. In fact, not only the protein and the membrane charges can be affected, but changes in association equilibria and molecular structure must also be considered (8, 9). These effects can be important for protein adsorption as well as for boundary limit layer polarization. The osmotic reduction of the applied pressure difference (Eqs. 2 and 4) also changes.

CONCLUSIONS

Permeability measurements for pure solvents and solutions under different conditions, made by using clean or pretreated membranes, allow for a full characterization of membrane transport and adsorption behavior.

BSA protein adsorbs on polyacrylonitrile membranes under both batch and ultrafiltration conditions. An adsorbed layer resistance, R_a , of the same order of magnitude as the resistance of the clean membrane, is produced. The effect is strongly dependent on solution pH and the maximum adsorption, and hence a higher membrane resistance is observed at the protein isolelectric point (pH 4.7).

In the design of a biopancreas that must produce and release insulin with a fixed time delay (less than 15 min) after an increase in the glucose level in blood (Fig. 1), the transport properties of the membranes are of fundamental importance for the kinetic behavior of the device.

REFERENCES

1. A. Suki, A. G. Fane, and C. J. D. Fell, "Flux Decline in Protein Ultrafiltration," *J. Membr. Sci.*, **21**, 269 (1984).
2. T. B. Choe, P. Masse, A. Verdier, and M. J. Clifton, "Membrane Fouling in the Ultrafiltration of Polyelectrolyte Solutions: Polyacrylic Acid and Bovine Serum Albumin," *Ibid.*, **26**, 17 (1986).
3. P. Aimar, S. Baklouti, and V. Sanchez, "Membrane-Solute Interactions: Influence on Pure Solvent Transfer during Ultrafiltration," *Ibid.*, **29**, 207 (1986).
4. G. Reach, M. Y. Jaffrin, and J-F. Desjeux, "A U-Shaped Bio-Artificial Pancreas with Rapid Lucose-Insulin Kinetics. In Vitro Evaluation and Kinetics Modelling," *Diabetes*, **33**, 752 (1984).
5. S. DiGiulio, C. Fabiani, G. Giubileo, and V. Violante, "The Bio-Artifical Endocrine Pancreas: Modelling and Performance Evaluation," *J. Membr. Sci.*, **36**, 541 (1988).
6. S. DiGiulio, C. Fabiani, G. Giubileo, and V. Violante, Pancreas endocrino bioartificiale. 1. Analisi di un modello in eometria cilindrica (Endocrine Bio-Artificial Pancreas. 1. Analysis of a Model with Cylindrical Geometry)," ENEA-RT/TIB/86/12, 1986.
7. S. DiGiulio, C. Fabiani, G. Giubileo, R. Noble, and V. Violante, *Analysis of a Implantable Bio-Artificial Pancreas for Insulin Production*, Presented at the First National Meeting NAMS, June 1987, Cincinnati, Ohio.
8. V. L. Vilker, C. K. Colton, and K. A. Smith, "The Osmotic Pressure of Concentrated Protein Solutions: Effect of Concentration and pH in Saline Solutions of Bovine Serum Albumin," *J. Colloid Interface Sci.*, **79**, 548 (1981).
9. V. L. Vilker, C. K. Colton, K. A. Smith, and D. L. Green, "The Osmotic Pressure of Concentrated Protein and Lipoprotein Solutions and Its Significance to Ultrafiltration," *J. Membr. Sci.*, **20**, 63 (1984).

10. W. Norde and J. L. Lyklema, "The Adsorption of Human Plasma Albumin and Bovine Pancreas Ribonuclease at Negatively Charged Polystyrene Surfaces. I. Adsorption Isotherms. Effect of Charge Ionic Strength and Temperature," *J. Colloid. Interface Sci.*, **66**, 257 (1978).
11. G. D. J. Phillies, G. B. Benedek, and N. A. Mazer, "Diffusion in Protein Solutions at High Concentrations: A Study by Quasi-Elastic Light Scattering Spectroscopy," *J. Chem. Phys.*, **65**, 1883. (1979).

Received by editor June 27, 1989